

# CFD-Based Study of Erosion Defects In Large Diameter Heating Bends

**Author: Xianliang Yang<sup>1</sup>; Jiayu Li<sup>2</sup>**

Affiliation: School of Energy, Power and Mechanical Engineering, North China Electric Power University, Hebei Province, China .

*E-mail: lijiaxu2633301441@163.com<sup>1</sup>; 2633301441@qq.com<sup>2</sup>;*

## ABSTRACT

*This paper firstly introduces the CFD theory of particle erosion, compares various turbulence models, and determines that the RNG model is used to control the fluid motion; the DPM model is used to control the particle motion.*

*When the particle mass flow rate is certain, the erosion effect of particles of different diameters on the bend is obtained, and the erosion rate of 90° bend is the largest, followed by that of 60° bend, and the erosion rate of 135° bend is the smallest. The same angle of the bend, the erosion rate with the increase in particle diameter shows a trend of first increase and then decrease. The position of the maximum erosion rate, that is, the most obvious erosion phenomenon of the region with the angle of the elbow decreases and gradually moved back. The erosion rate of the pipe increases with the increase of particle number, and the two curves approximate a function; the erosion rate of the pipe increases with the increase of hot water flow rate in the pipe. When the mass flow rate of particles is certain, the erosion phenomenon of pipeline is most serious for particles with 200μm diameter, and the maximum erosion rate appears in the case of particle flow rate of 0.2kg/s and flow rate of 3.0m/s.*

**Keywords: bend tube erosion; CFD simulation; solid-liquid two-phase flow; erosion rate**

## 1. INTRODUCTION

Pipelines play a very important role in urban central heating projects, and the reliability of pipeline networks has been the focus of scholars at home and abroad. Although the hot water in the pipeline has been softened and desanded, it will inevitably carry a small amount of sand into the

pipeline network, and the flow of solid sand in the pipeline will inevitably have an erosion effect on the pipeline and its accessories, thus causing wear and tear of the pipeline and its accessories to affect the reliability of the pipeline [1]. The flow direction of sand grains suddenly changes at the bend, while the influence of secondary flow produces obvious changes in velocity magnitude and direction, so the bend is the most serious part of the erosion [2]; however, there are many factors affecting the flow law of solid-liquid two-phase flow in the bend, and the study of the erosion mechanism of the pipe wall is a complex problem [6].

Researchers at home and abroad have done a lot of work for the scour corrosion of pipes, and the main research methods include computational fluid dynamics (CFD) simulation of bend erosion [7,8], bend erosion experiments [9-11], and establishment of pipe erosion models [12-14]. Mansouria studied the erosion of bends by different types of fine sand at different velocities, and improved CFD method to calculate the erosion of bends by sand particles [16]. Mansouria studied the erosion of bends by different types of fine sand at different velocities and improved CFD method to calculate the erosion of bends by sand particles [16]. Yanhua Wang [17] and Ying Lu [6] used numerical simulation methods to study the factors influencing the location of occurrence and erosion rate of scour corrosion of bends by solid-liquid two-phase flow. Most of the previous work focused on the petrochemical field to study oil and gas transmission pipelines, while the working medium and working conditions of heating pipelines and oil pipelines are completely different, and the study of scouring corrosion of bends for large pipe diameters is not perfect. This paper establishes a numerical model of liquid-solid flow for the fluid

characteristics in large diameter heating bends, and studies the influence of different factors on the bend erosion, so as to provide reference for the design of heating pipes and heating regulation.

Hot water and sand particles flow mixed in the heating pipe, and its calculation model is a complex liquid-solid two-phase flow model, with hot water as the continuous phase and sand particles as the discrete phase. In the process of solid-liquid two-phase flow, collision occurs between the particles, and there is interaction between the particles and the liquid phase, and the particles hit the pipe wall and are bounced off. The main consideration for calculating the erosion of sand particles on the bend is the movement of continuous and discrete phases in the bend and the collision of particles on the wall of the pipe.

## 2. MODEL

### 2.1 Continuous phase control equation

As a three-dimensional, incompressible fluid, the flow of the continuous phase follows conservation of mass and conservation of momentum, whose governing equations are the continuous equation and the Navier-Stokes momentum equation, respectively, expressed as follows:

Continuous equation:

$$\frac{\partial \rho}{\partial t} + \frac{\partial \rho u_i}{\partial x_i} = 0 \quad (1)$$

Momentum equation:

$$\frac{\partial \rho u_i}{\partial t} + \frac{\partial}{\partial x_j} (\rho u_i u_j) = -\frac{\partial p}{\partial x_i} + \frac{\partial}{\partial x_j} \left[ (\mu + \mu_t) \left( \frac{\partial u_i}{\partial x_j} + \frac{\partial u_j}{\partial x_i} \right) \right] \quad (2)$$

Generally the flow state of the fluid is divided into laminar and turbulent flow, and the fluid flow considered in this paper has a Reynolds number of roughly  $Re = 2.5 \times 10^6$  for the turbulent flow state. The fluid flow in the bend is accurately calculated using the  $k-\varepsilon$  model. The RNG  $k-\varepsilon$  model used in this paper adds one more condition to the  $\varepsilon$  equation compared with other models of the  $k-\varepsilon$  model, and takes into account the vortex generated by the fluid flow, so it has a higher accuracy.

### 2.2 Discrete phase control equations

The motion of the discrete phase is controlled by the Euler-Lagrange method, which takes into account the particle-fluid interaction, i.e., the momentum, mass, and energy exchange between the particles and the fluid. In the flow field, the forces on the discrete phase in the Lagrangian coordinate system and its motion follow Newton's second law. The researchers found that particle-particle collisions can be neglected when the volume fraction occupied by the particles in the pipe is small, so the interaction between particles in the discrete phase is not considered in this paper.

### 2.3 Wall recovery equation

The particles inside the bend collide with the inner wall of the bend and are bounced off; since the collision form is inelastic, a part of the energy of the particles is lost in this process, which means that the velocity of the particles decreases to some extent after the collision, and their velocity direction also changes. The energy loss when the particle collides with the wall can be better studied by calculating the ratio of the velocity components of the particle before and after the collision, which are defined as the normal recovery coefficient  $e_n$  and the tangential recovery coefficient  $e_t$ , respectively.

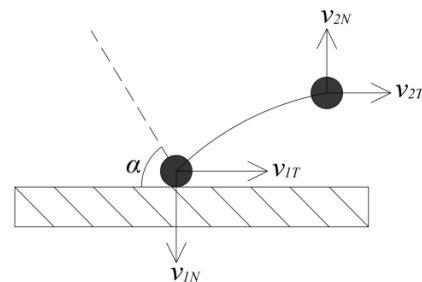


**Fig. 1 Schematic diagram of particle bounce**

In this paper, the wall bounce recovery coefficient uses the expression proposed by Grant and Tabakoff.

### 2.4 Erosion model

The McLaury erosion model is well suited for solid-liquid two-phase flow and is mainly used to simulate the erosion rate of sand-bearing water on the pipe. Considering that the impact angle of particles has a significant effect on the erosion rate, McLaury also proposed an impact angle function

applicable to his own erosion model; at the particle impact velocity less than 10 m/s, the erosion rate of sandy water flow on carbon steel pipe wall is expressed as :

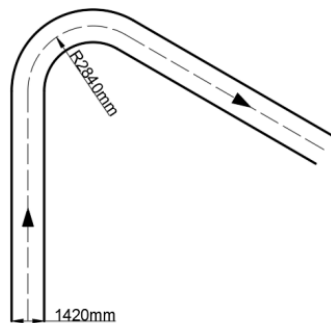
$$R_e = \sum_{p=1}^N \frac{m_p C(d_p) f(\alpha) v^{b(v)}}{A_f} \quad (3)$$

In the formula : $R_e$  Erosion rate;  $N$ , The total number of particles on the impact wall;  $m_p$  , The mass flow rate of solid particles impacting the wall;  $C(d_p)$ , Particle size function;  $f(\alpha)$ , Particle path as a function of wall impact angle; $b(v)$  , Particle relative velocity function;  $A_f$ , Wall area.

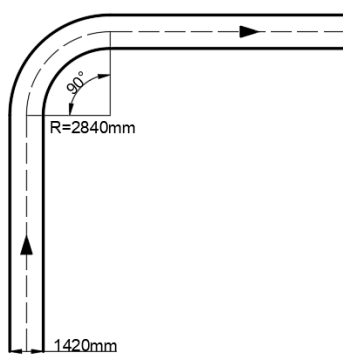
### 3. NUMERICAL SIMULATION

#### 3.1 Pipe geometry model

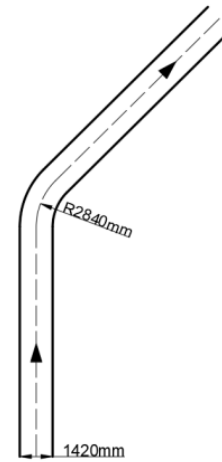
The main research object of this section is the elbow with different angles of DN1400 caliber. The bending radius of the elbow is set as 2D. In order to ensure that the fluid in the pipe fully develops into a turbulent state, the length of the straight pipe section connected with the elbow is set as 10m. Fig. 2 shows the specific geometric dimensions.



(a) 60° bend pipe



(b) 90° bend pipe



(c) 135° bend pipe

**Fig. 2 Structure diagram of bending pipe with different angles**

#### 3.2 Model grid division

The Meshing module was used to divide the three kinds of bending pipes into unstructured grids, and the mesh encryption was carried out for the elbow part to improve the calculation accuracy. Considering that the flow state of hot water in the pipeline is turbulent, and the part close to the pipe wall is boundary layer, which is generally millimeter or even micron. Therefore, in order to reduce the number of grids and reduce the calculation workload, the first layer of grids can be placed in the core region of turbulence, and the  $y+$  value is set at 100, the height of the first layer of grids can be calculated as 0.8mm. At the same time, the number of expansion layers is set to 10, and the growth rate is 1.1. The grid division of 90° bending pipe is shown in Fig. 3:

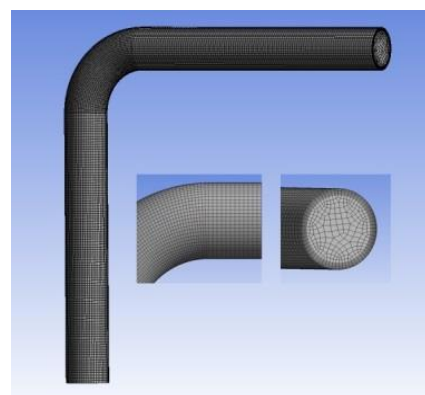


**Fig. 3 Grid division of 90° bend pipe**

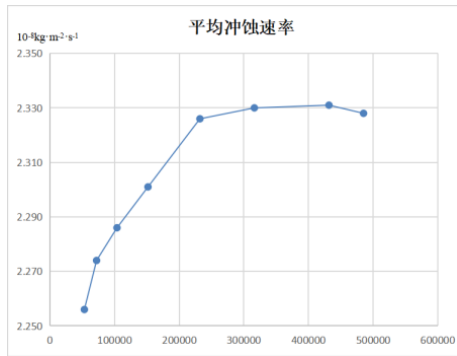


**Fig. 4. Average erosion rate under different mesh quantities**

When using Fluent to conduct CFD simulation, excellent grid division has a very important impact on the calculation results and calculation time. In order to fully ensure the accuracy of the simulation results and reduce the workload, grid independence testing should be carried out. The main operation is to find the minimum number of grids independent of the CFD calculation results. As shown in Fig. 4, a total of 8 groups of different grid numbers are set. It can be seen that when the number of grids is less than 200,000, the average erosion rate of solid particles on the pipeline is low and has no reliability. When the number of grids reaches 300,000, the numerical simulation results tend to be stable, and the calculation results slightly decrease as the number of grids further increases to more than 500,000. Therefore, it can be concluded that the calculation results are stable and reliable when the number of grids is between 300,000 and 500,000. Therefore, the division method with the number of grids as 316204 is selected.

### 3.3 Setting boundary conditions

The continuous phase was set as liquid water, and the flow rate was set as 3m/s according to the maximum design flow rate of heating pipe. The discrete phase was set as sand particle, the density was 2650kg/m<sup>3</sup>, and the particle size was set as 50μm, 100μm, 200μm, 500 and 1mm, respectively. The pipe material is Q235 steel with a density of 2650kg/m<sup>3</sup>.

The model inlet was set as velocity inlet, with pressure of 1.6MPa, turbulence intensity of 2.37%, and characteristic length of 1.42m. outflow is set to outflow. The RNG k-ε model is used to simulate the continuous phase turbulence in the flow field, and the expandable wall penalty function condition is selected to better simulate the boundary layer flow in the flow field. The motion of discrete phase

is controlled by DPM model, and the following assumptions should be made: 1) The interaction between sand particles should be ignored; 2) Sand particles are uniformly released from the pipe entrance; 3) The shape of sand grains is regarded as a sphere; 4) The release rate of sand is consistent with that of fluid. The inlet and outlet of the pipeline were set as the escape boundary, and the wall was set as the reflect boundary. Inelastic collision occurred between the particle and the wall surface, and the wall recovery coefficient was adopted by formula 5.

In the solver setting, the pressure-velocity coupling method was SIMPIE method, and the pressure gradient was PRESTO! Methods, other parameters were set to the second-order upwind scheme, and the isothermal steady-state condition was used to solve the problem. The number of iteration steps is set to 1500, and the convergence standard is set to 10<sup>-5</sup>.

## 4. SIMULATION RESULTS AND ANALYSIS

In the pipeline system, due to the special geometric structure of the elbow, the fluid suddenly turns here, and the elbow bears the direct impact of solid particles on it. Therefore, compared with other parts of the pipeline system, the elbow is more vulnerable to erosion damage by particles. In this paper, three common Angle models of elbow of 60°, 90° and 135° are set first. The flow field distribution in the curved pipe with different angles was analyzed to determine the flow characteristics of the two-phase flow and the erosion rule of the particles relative to the curved pipe with different angles. Then, the influence of different factors on the erosion of the curved pipe was studied by setting different particle velocity, size and flow rate.

### 4.1 Flow field distribution of bent pipes at different angles

In this paper, the bending pipe models with different angles were established. The fluid flow rate in the pipe was 3m/s, the working pressure was 1.6MPa, and the mass flow rate of particles was 0.2kg/s. The particles were regarded as regular spheres with diameters of 50μm, 100μm, 200μm, 500 and 1mm, respectively. Firstly, the velocity and pressure distribution of the flow field in different pipelines are analyzed to obtain the fluid flow state in the pipeline, and then the impact

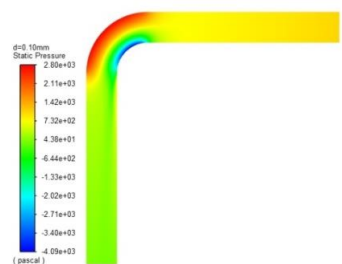
effect of particles on the inner wall of the pipeline is analyzed.

#### 4.1.1 Pressure distribution

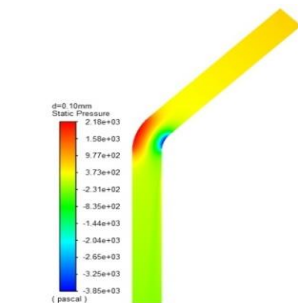
By comparing the simulation results of bending pipes with different angles, it can be concluded that when the particle size of sand is different, the pressure distribution in the bending pipe with the same Angle does not change significantly. Therefore, it can be concluded that when the mass flow rate of sand is constant, the particle size of sand has no effect on the pressure distribution of fluid in the pipe. Therefore, one of the following situations is selected for discussion and analysis to study the influence of elbow Angle on pressure distribution. Since the working pressure of the pipeline is 1600000Pa, the pressure caused by fluid flow is within the range of 1596000 Pa-1603000Pa, which is difficult to accurately represent in the cloud image due to the small variation range. Therefore, static pressure is used to represent the pressure change in the pipeline.



(a) 60° bend pipe



(b) 90° bend pipe



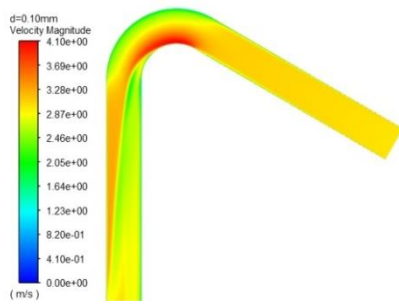
(c) 135° bend pipe

**Fig. 5 Pressure (static pressure) distribution nephogram in curved tubes at different angles**

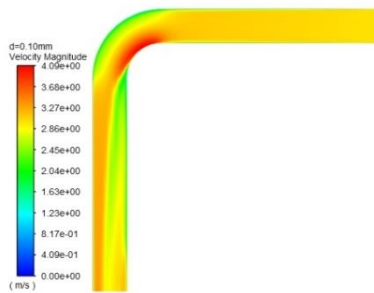
Fig. 5 shows the distribution nephogram of static pressure in the 60°, 90°, and 135° bends when the particle diameter is 100 $\mu$ m. According to the pressure distribution nephogram in Fig. 5, when the liquid-solid two-phase flow enters the straight pipe section of the inlet of the bend, the flow direction decreases gradually, and the pressure changes obviously after entering the bend. There is an obvious gradient change in the direction from the inner arch to the outer arch. The pressure near the outer arch is the maximum, while the pressure near the inner arch is the minimum. The pressure change becomes slow again when the outflow elbow enters the outlet straight pipe section. The pressure of the three elbows varies from -4000 Pa to 3000 Pa, and the maximum pressure on the 60° side of the outer arch reaches 2960Pa. The maximum pressure on the inner arch side of 90° elbow is 2830 Pa; The pressure value of the outer arch of 135° elbow is 2180Pa, which is the lowest among the three kinds of elbow angles, and the minimum pressure value of one side of the inner arch of the three kinds of elbow is about -4000 Pa. It can be concluded that the pressure drop of 60° elbow is the largest, followed by 90° elbow and 135° elbow. The pressure change of the fluid flowing through the elbow is related to the Angle of the elbow, the smaller the Angle of the elbow, the more obvious the pressure change degree.

#### 4.1.2 Velocity Distribution

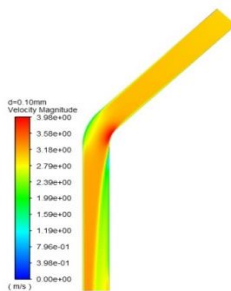
The movement of particles in the pipe is complicated, because the particles exchange momentum and mass with the fluid during the movement, and the flow state is affected by the interaction between the particles and the fluid. To understand the motion of particles, one must first analyze the flow of fluids. By comparing the simulation results of different Angle bending pipes, it can be concluded that when the particle size of the sand is different, the velocity distribution in the same Angle bending pipe does not change significantly and all are within the range of 0-4.0m/s, because the particle concentration and size are small and have little influence on the fluid. Therefore, it can be concluded that when the mass flow rate of sand is constant, the particle size of sand has no effect on the fluid pressure distribution in the pipeline.



(a) 60° bend pipe



(b) 90° bend pipe



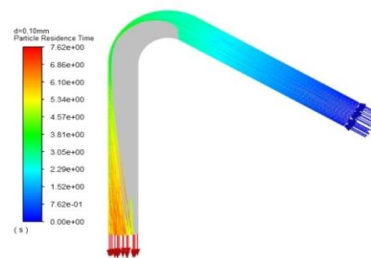
(c) 135° bend pipe

**Fig. 6 Velocity distribution nephogram in different angles**

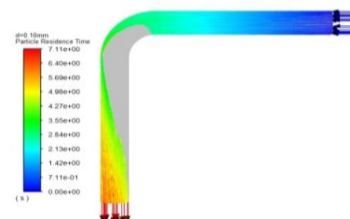
As shown in Fig. 6, the velocity of sand particle and fluid at the entrance of the pipeline is the same, while the velocity in the turbulent core area hardly changes when entering the straight pipe section of the entrance. Only the velocity near the wall decreases significantly. After entering the elbow, the velocity changes become obvious, and the velocity decreases rapidly. After entering the outlet straight pipe section, the velocity increases to some extent, and a more obvious gradient distribution appears. This is because sand particles collide with the pipe wall at the elbow, which is also the main reason that solid particles in the pipe will cause erosion to the pipe wall. It can also be concluded that the velocity at the outer arch wall of the elbow

is significantly lower than that at the inner arch wall of the elbow.

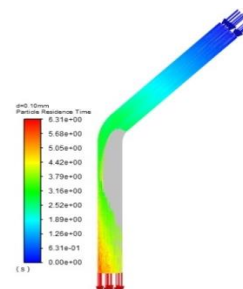
As can be seen from Fig. 7, sand particles are evenly distributed in the straight pipe section at the entrance. When reaching the elbow, sand particles are mainly concentrated in the outer arch of the elbow, and gradually distributed in the whole pipe after flowing out of the elbow. Since there is almost no sand in the inner arch of the elbow, the fluid does not need to drive the sand flow, and the kinetic energy loss of the fluid is small, so the fluid speed is larger. However, the outer arch of the elbow is exactly the opposite. Since particles are mainly distributed in the outer arch area when flowing through the elbow, momentum exchange between the fluid and particles in the outer arch area is more frequent, so the kinetic energy loss is also larger. The velocity of the fluid will decrease significantly.



(a) 60° bend pipe



(b) 90° bend pipe



(c) 135° bend pipe

**Fig. 7 Particle trajectories in curved tubes with different angles**

Combined with the pressure and velocity distribution of flow fields inside different bends, it can be concluded that the flow of sand-carrying water flowing into the bend section will change significantly. The fluid is affected by the curvature of the bend and generates a transverse pressure gradient, resulting in the maximum velocity gradually moving to the position of the inner arch wall of the bend. When the fluid flows out of the bend and enters the outlet straight pipe section, the pressure gradient disappears. The maximum velocity will move to the outer wall of the pipe.

#### 4.2 Erosion law of bending pipe at different angles

As shown in Fig. 8, when solid particle diameter  $d=50\mu\text{m}$ , particle flow rate is  $0.2\text{kg/s}$ , and particle release velocity is  $3\text{m/s}$ , erosion rate is used to reflect the simulation results of particle erosion on bent pipes at various angles.

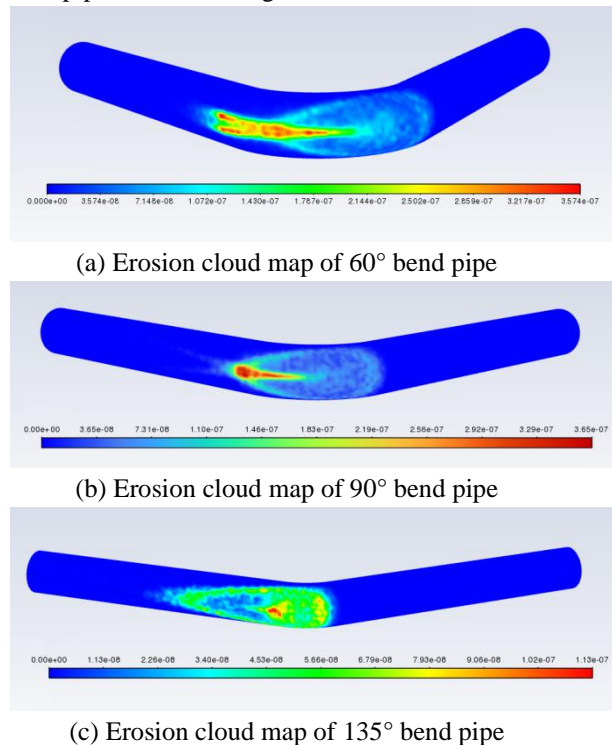


**Fig. 8 Cloud diagram of erosion rate of bending pipe at different angles when  $d=50\mu\text{m}$**

It can be seen from Fig. 8 that other parameters remain unchanged. When the particle diameter is  $0.05\text{mm}$ , the most serious locations of sand erosion of the three kinds of bend pipes are all distributed near the horizontal center line of the inner wall of the outer arch of the bend. The erosive wall area of the 90° bend is the smallest and concentrated in the elbow area. The erosive position of the 60° and 135° bend includes not only the elbow area but also

part of the outlet straight pipe section connected to the elbow. The erosive avoidance area is relatively large.

The maximum erosion rate of particles on the 135° bend is  $1.13 \times 10^{-7} \text{kg}/(\text{m}^2 \cdot \text{s})$ . There is little difference between the maximum erosion rate of particles on the 60° bend and the 90° bend, but the value is about 3 times that of the 135° bend. Therefore, it can be inferred that the erosion phenomenon of the 135° bend is lighter under the same circumstances.

As shown in Fig. 9, when solid particle diameter  $d=100\mu\text{m}$ , particle flow rate is  $0.2\text{kg/s}$ , and particle release velocity is  $3\text{m/s}$ , erosion rate is used to reflect the simulation results of particle erosion on bent pipes at various angles.

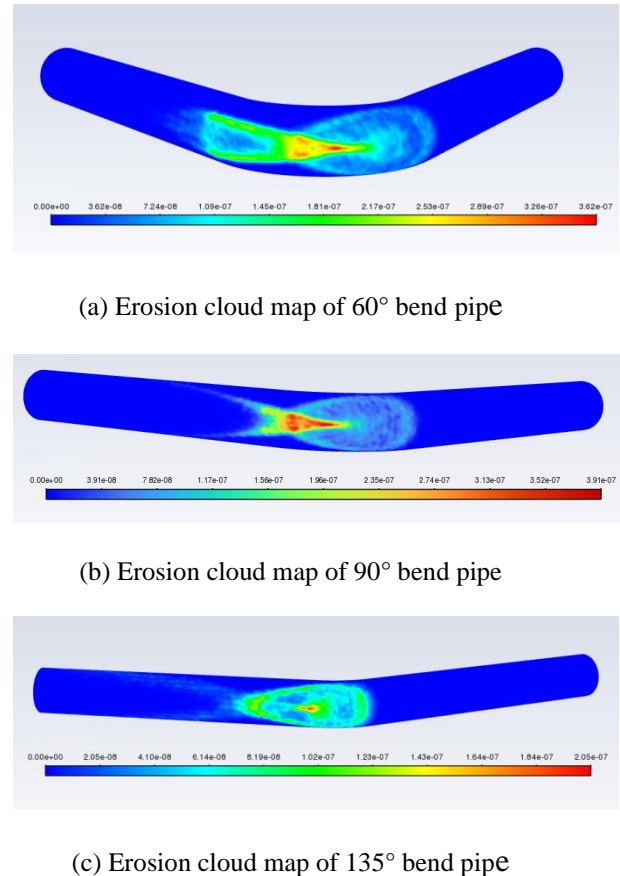
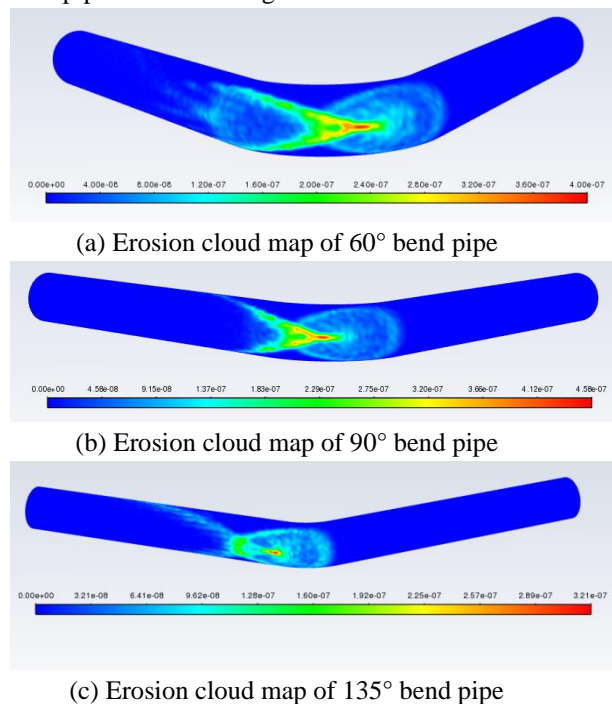


**FIG. 9 Cloud diagram of erosion rate of bending pipe at different angles when  $d=100\mu\text{m}$**

Compared with the results in Fig. 7, it can be found that when the particle diameter increases to  $100\mu\text{m}$ , the erosion rate of the three kinds of pipe increases. The erosion rate increment of the 60° pipe is only  $0.05 \text{ kg}/(\text{m}^2 \cdot \text{s})$ , and that of the 90° pipe is  $0.26 \text{ kg}/(\text{m}^2 \cdot \text{s})$ . The erosion rate of 135° bend reaches  $2.05 \text{ kg}/(\text{m}^2 \cdot \text{s})$ , which is nearly doubled. However, the most serious area of particle erosion on the elbow

moves slightly towards the entrance of the elbow. The main reason is that with the increase of particle diameter, the weight of a single particle also increases. Therefore, the carrying capacity of the particle by the water flow decreases, resulting in the collision between the particle and the wall near the entrance of the elbow.

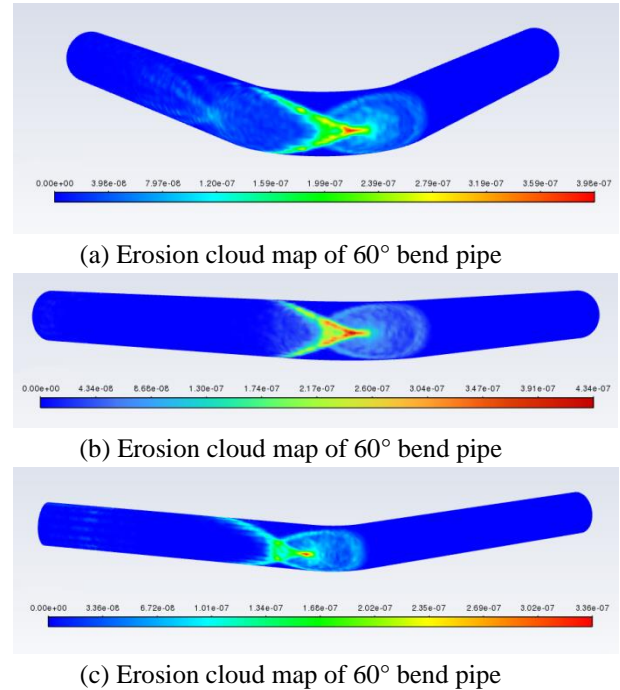
As shown in FIG. 10, when solid particle diameter  $d=200\mu\text{m}$ , particle flow rate is  $0.2\text{kg/s}$ , and particle release velocity is  $3\text{m/s}$ , erosion rate is used to reflect the simulation results of particle erosion on bent pipes at various angles.



**Fig. 10 Cloud diagram of erosion rate of bending pipe at different angles when  $d=200\mu\text{m}$ .**

With the increase of particle diameter to  $200\mu\text{m}$ , the erosion rate of particles on the tube increases again, but the erosion rate of  $135^\circ$  tube is still the lowest, and the erosion rate of  $90^\circ$  tube is the highest. At the same time, it is found that the areas with the most serious erosion of the three kinds of bend pipe, namely the red areas in the cloud map, all decrease. The reason is that particle diameter increases, but particle mass flow rate remains unchanged, and the number of particles in the pipe decreases obviously, so the probability of particle collision with the pipe decreases, resulting in the decrease of collision area. However, as the particle size increases, the kinetic energy of a single particle also increases, so the erosion phenomenon of particles on the tube wall is more obvious as the erosion rate increases.

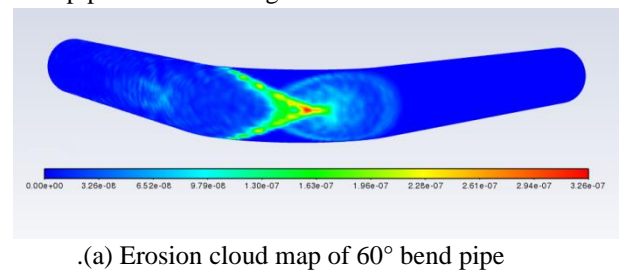
As shown in Fig. 11, when solid particle diameter  $d=500\mu\text{m}$ , particle flow rate is  $0.2\text{kg/s}$ , and particle release velocity is  $3\text{m/s}$ , erosion rate is used to reflect the simulation results of particle erosion on bent pipes at various angles.

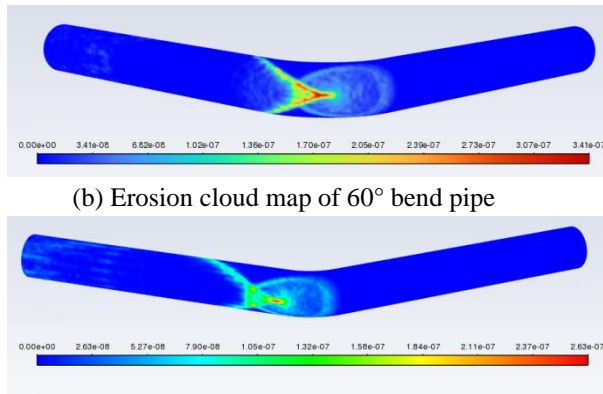


**Fig. 11  $d=500\mu\text{m}$  erosion rate cloud diagram of bending pipe at different angles**

When the particle diameter reached  $500\mu\text{m}$ , the most serious erosion area of the bend was further reduced, and the position moved to the entrance of the bend again. However, the maximum erosion rate of particles on the  $60^\circ$  and  $90^\circ$  bending tubes did not increase again but gradually decreased, and the erosion rate of particles on the  $135^\circ$  bending tubes continued to increase but the growth rate slowed down.

As shown in Fig. 12, when solid particle diameter  $d=1\text{mm}$ , particle flow rate is  $0.2\text{kg/s}$ , and particle release velocity is  $3\text{m/s}$ , erosion rate is used to reflect the simulation results of particle erosion on bent pipes at various angles.





(b) Erosion cloud map of 60° bend pipe

(c) Erosion cloud map of 60° bend pipe

**Fig. 12 Cloud map of erosion rate of bending pipe at different angles when d=1mm**

When the diameter of particles in the pipe is 1mm, the weight of individual particles increases further, and the influence of water flow on particles decreases further. It can be found that the maximum erosion rate of the three curved pipes is in a decreasing trend, and the erosion area is also decreasing. Therefore, it can be considered that when the mass flow rate of particles is constant, the particle diameter has a critical value. Before reaching this critical value, the erosion rate of particles on the elbow increases with the increase of particle diameter; when exceeding this critical value, the erosion rate decreases gradually.

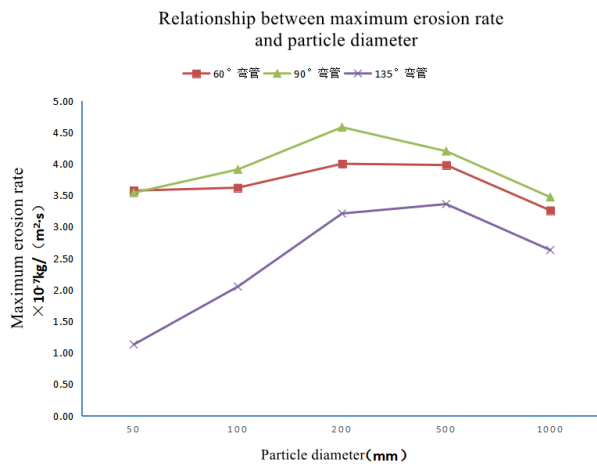


**Fig. 13. The relationship between the maximum erosion rate and particle diameter**

According to Fig. 13, the erosion laws of bending pipes with different angles can be concluded as follows: 1) When the particle diameter is fixed, the erosion rate of bending pipe with 90° is the highest, followed by that of bending pipe with 60°, and that of bending pipe with 135° is the lowest. 2) For a curved pipe with the same Angle, when the particle diameter gradually increases, the erosion rate increases first and then decreases. Therefore, it can

be inferred that there is a critical value. When the particle diameter reaches this critical value, the erosion phenomenon on the curved pipe is the most obvious.

### 4.3 Influence of particle quantity on erosion of 90° bend pipe.

The direct parameter that affects the number of particles is the mass flow rate of particles. In order to study the influence of the number of particles on the erosion of the 90° bend pipe, the above physical model of the 90° bend pipe is still adopted in the pipeline model. The diameter of particles is 200μm, and the mass flow rate of particles is set as 0.04kg/s, 0.08kg/s and 0.12kg/s respectively. 0.16kg/s, 0.20kg/s, other parameters and Settings remain unchanged for simulation calculation.

As can be seen from Fig. 14, when other conditions remain unchanged, the maximum erosion rate of the bend increases with the increase of particle mass flow rate, and the two can be fitted into a linear curve:  $Re=0.9166q-0.027$ . Therefore, according to the set mass flow rate of five kinds of particles, when the particle flow rate is 0.20 kg/s, the maximum erosion rate is  $4.58 \times 10^{-7}$  kg/ (m<sup>2</sup>·s), and the erosion rate multiplied by the pipe material density can be converted into the pipe wall thinning thickness of 0.005mm/day.

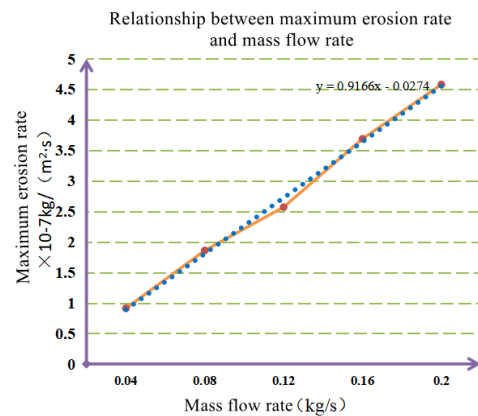


**Fig. 14 Relation between particle mass flow rate and maximum erosion rate**

### 4.4 Influence of particle diameter on erosion of 90° bend pipe

After the above erosion simulation results under different particle diameters were sorted out, when particle mass flow rate  $q=0.2$ kg, particle velocity was 3m/s, and particle diameters were  $d=0.05$ mm,  $d=0.1$ mm,  $d=0.2$ mm,  $d=0.5$ mm,  $d=1.0$ mm, the

variation law of pipeline erosion rate with particle diameters was shown in Fig. 15.

It can be analyzed that when the particle velocity and mass flow rate are fixed, the erosion rate of particles on the pipe does not simply increase with the increase of particle diameter, but first increases and then decreases, which indicates that there is a particle diameter that is most serious to the pipe erosion. According to Fig. 15, the critical value of this diameter should be around 0.2mm.

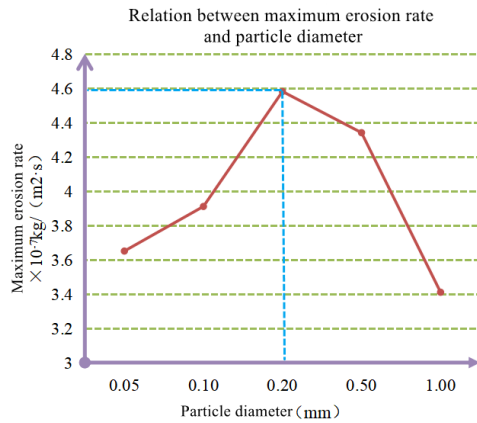


**Fig. 15** Relation between 90° particle diameter and maximum erosion rate

#### 4.5 Influence of flow rate on erosion of 90° bend pipe

In order to study the influence of particle velocity on the erosion of curved pipe, we can indirectly set the change of hot water velocity to represent the change of particle velocity, because the movement of particles in the pipe is directly affected by the movement of hot water. Considering that the actual flow rate of hot water pipe is generally below 3.0m/s, the flow rate of medium in the pipe is set as 1.0m/s, 1.5m/s, 2.0m/s, 2.5m/s, 3.0m/s, and other parameters and Settings remain unchanged.

Fig. 16 shows the relationship between particle velocity and maximum restatement rate of elbow. It can be seen that a conic curve can be synthesized according to the five points corresponding to the five flow rates set:  $Re=0.135v^2+0.215v+0.114$ . The maximum erosion velocity of pipeline gradually increases with the increase of particle velocity, which is because liquid provides a drag force for particles to move with liquid. With the increase of medium velocity, kinetic energy of particles will also increase, so the impact on pipeline becomes more serious, and the loss of pipeline materials, that is, the erosion amount of pipeline, will also increase.

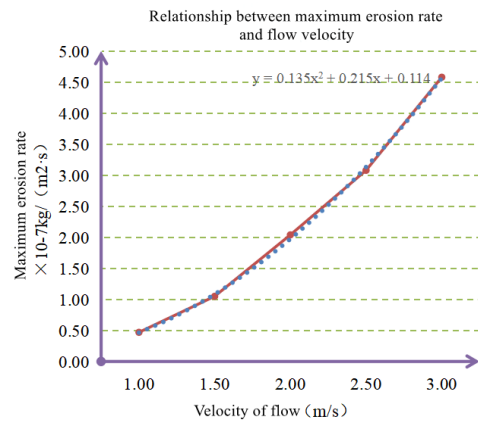


**Fig. 16** Relation between particle velocity and maximum erosion rate

## 5. CONCLUSION

1. Through the analysis of the flow field of the elbow with different angles, it is concluded that the pressure change is very obvious when the fluid flows through the elbow. The maximum pressure position of the three kinds of elbow is on the inner wall of the elbow and the outer arch side, and the pressure change degree of the elbow decreases with the increase of the elbow Angle. The maximum velocity in the flow field is distributed on one side of the inner arch of the elbow. When the particle concentration is low, the particle diameter has little effect on the pressure and velocity distribution in the flow field.

2. By comparing the erosion effect of particles of different diameters on the pipe when the mass flow rate of particles is constant, it is concluded that the erosion rate of 90° pipe is the highest, followed by that of 60° pipe, and that of 135° pipe is the lowest. The erosion rate of the curved pipe with the same Angle increases first and then decreases with the increase of particle diameter. The reason is that as the particle diameter increases, the number of particles will decrease, so the frequency of particle collisions with the tube wall will decrease. As the Angle of the elbow decreases, the area where the erosion rate is maximum, namely the area where the erosion phenomenon is most obvious, gradually moves backward.

3. By setting the influence of different particle quantity and hot water velocity on the erosion rate of the 90° bend pipe, it is concluded that the erosion rate of the pipe increases with the increase of particle quantity, and the curves of the two curves are approximate to the first function; The erosion rate increases with the flow rate of hot water in the pipe. When the mass flow rate of

particles is constant, the erosion phenomenon of particles with diameter of 200 $\mu$ m is the most serious. The maximum erosion rate occurs when the particle flow rate is 0.2kg/s and the flow rate is 3.0m/s.

## 6. REFERENCES

- [1]. Chen Wenhao, Zhang Shishui, Gao Rui, et al. Particle movement and Blade wear of inclined Flow Pump in Deep Sea Mining [J]. Journal of Drainage and Irrigation Machinery Engineering, 20, 38(12) : 1215-1220.
- [2]. Zhao Ruijie, Zhao Youlong, Zhou Lu, Zhang Desheng. Numerical Simulation of Coarse Particle Wear Characteristics of Solid-liquid Two-phase Flow in 90° Curved Pipe [J]. Journal of Huazhong University of Science and Technology (Natural Science Edition), 201,49(10):47-52+66.
- [3]. Patrick Frawley et al. Combination of CFD and DOE to analyse solid particle erosion in elbows[J]. International Journal of Computational Fluid Dynamics, 2009, 23(5) : 411-426.
- [4]. Kai, LI Xiufeng, WANG Yue-she, Chen Yanlin, HAN Shuang, HE Ren-Yang. Prediction of position of solid particles on erosion failure of curved pipe in liquid-solid two-phase flow [J]. Chinese Journal of Engineering Thermophysics, 2014,35(04):691-694.
- [5]. Zahedi P , Parsi M , Asgharpour A , et al. Experimental investigation of sand particle erosion in a 90° elbow in annular two-phase flows[J]. Wear, 2019, 438-439:203048.
- [6]. Lu Ying, MA Guiyang. Numerical Simulation of Liquid-Solid Two-Phase Scour Corrosion in  $\pi$ -type Pipe [J]. Journal of Liaoning Shihua University, 2021,41(04):52-57.
- [7]. Peng Wenshan, Cao Xuewen. Erosion effect of solid particles on liquid/Solid Two-phase Flow Pipe [J]. Chinese Journal of Corrosion and Protection, 2015,35(06):556-562.
- [8]. Jia-wei Zhou et al. Effects of particle shape and swirling intensity on elbow erosion in dilute-phase pneumatic conveying[J]. Wear, 2017, 380-381 : 66-77.
- [9]. Zeng Li. Erosion Corrosion Mechanism and Fluid Dynamics Characteristics of Pipe Bend [D]. Huazhong University of Science and Technology,2017.
- [10]. Lei Xu et al. Numerical prediction of erosion in elbow based on CFD-DEM simulation[J]. Powder Technology, 2016, 302 : 236-246.
- [11]. Huang Shaopu. Study on the Erosion Characteristics of Liquid-Solid Two-Phase Flow on Curved Pipe [D]. Xi 'an Shiyou University,2020.
- [12]. Practical estimation of erosion damage caused by solid particle impact[J]. Wear, 2005, 259(s 1–6):95-101.
- [13]. Zhang Y , Reuterfors E P , Mclaury B S , et al. Comparison of computed and measured particle velocities and erosion in water and air flows[J]. Wear, 2007, 263(1-6):330-338.
- [14]. Pereira G C , Souza F , Martins D . Numerical prediction of the erosion due to particles in elbows[J]. Powder Technology, 2014, 261(7):105–117.
- [15]. Mazdak Parsi et al. CFD simulation of sand particle erosion in gas-dominant multiphase flow[J]. Journal of Natural Gas Science and Engineering, 2015, 27 : 706-718.
- [16]. Mansouria A, Arabnejad H, Karimi S, et al. Improved CFD modeling and validation of erosion damage due to finesand particles [J] .Wear, 2015, 338-339: 339-350.
- [17]. Wang Yanhua, Wu Yuguo, Zhang Shaochuan, Zhang Wanying. Numerical Simulation of Erosion Corrosion of  $\pi$ -type Pipe [J]. Surface Technology, 20,49(12):259-266.